

Mind the GAP! The Challenges of Scale in Pixel-based Deep Reinforcement Learning

Ghada Sokar¹ and Pablo Samuel Castro¹

¹Google DeepMind

Scaling deep reinforcement learning in pixel-based environments presents a significant challenge, often resulting in diminished performance. While recent works have proposed algorithmic and architectural approaches to address this, the underlying cause of the performance drop remains unclear. In this paper, we identify the connection between the output of the encoder (a stack of convolutional layers) and the ensuing dense layers as the main underlying factor limiting scaling capabilities; we denote this connection as the bottleneck, and we demonstrate that previous approaches implicitly target this bottleneck. As a result of our analyses, we present global average pooling as a simple yet effective way of targeting the bottleneck, thereby avoiding the complexity of earlier approaches.

1. Introduction

Reinforcement learning (RL) is widely considered one of the most effective approaches for complex sequential decision-making problems (Bellemare et al., 2020; Degraeve et al., 2022; Mnih et al., 2015; Vinyals et al., 2019; Wurman et al., 2022), in particular when combined with deep neural networks (typically referred to as deep RL). In contrast to the so-called “scaling laws” observed in supervised learning (where larger networks typically result in improved performance), it is difficult to scale RL networks without sacrificing performance. There has been a recent line of work aimed at developing techniques for effectively scaling value-based networks, such as via the use of mixtures-of-experts (Obando Ceron* et al., 2024), network pruning (Obando Ceron et al., 2024), tokenization (Sokar et al., 2025), and regularization (Nauman et al., 2024). These techniques tend to focus on structural modifications to standard deep RL networks by leveraging sparse-network training techniques from the supervised learning literature.

Obando Ceron* et al. (2024) first demonstrated that naïvely scaling the penultimate (dense) layer in an RL network results in *decreased* performance, and proposed the use of soft mixtures-of-experts (SoftMoEs; Puigcerver et al., 2024) to enable improved performance from this form of scaling. Sokar et al. (2025) argued that the gains from SoftMoEs were mostly due to the use of tokenization. Relatedly, Obando Ceron et al. (2024) demonstrated that naïvely scaling the convolutional layers hurts performance, and showed that incremental parameter pruning yields gains that grow with the size of the original, unpruned, network. While effective, all these methods are non-trivial to implement and can result in increased computational costs.

One unifying aspect of the aforementioned works is that they tend to be most effective on networks that process pixel inputs, such as when training on the ALE (Bellemare et al., 2013). These networks are typically divided into an *encoder* ϕ consisting of a series of convolutional layers, followed by a series of dense layers ψ ; thus, for an input x , the network output is given by $\psi(\phi(x))$. Obando Ceron* et al. (2024) and Sokar et al. (2025) scaled the first layer of ψ while Obando Ceron et al. (2024) scaled all layers in ϕ . It is worth highlighting that $\psi \circ \phi$ is, in practice, a set of weights connecting the output of $\phi(x)$ with the input layer of ψ .

In this work, we argue that the underlying cause behind the effectiveness of the aforementioned methods is that they result in a **bottleneck** between $\phi(x)$ and ψ (see Figure 1). As we will argue,

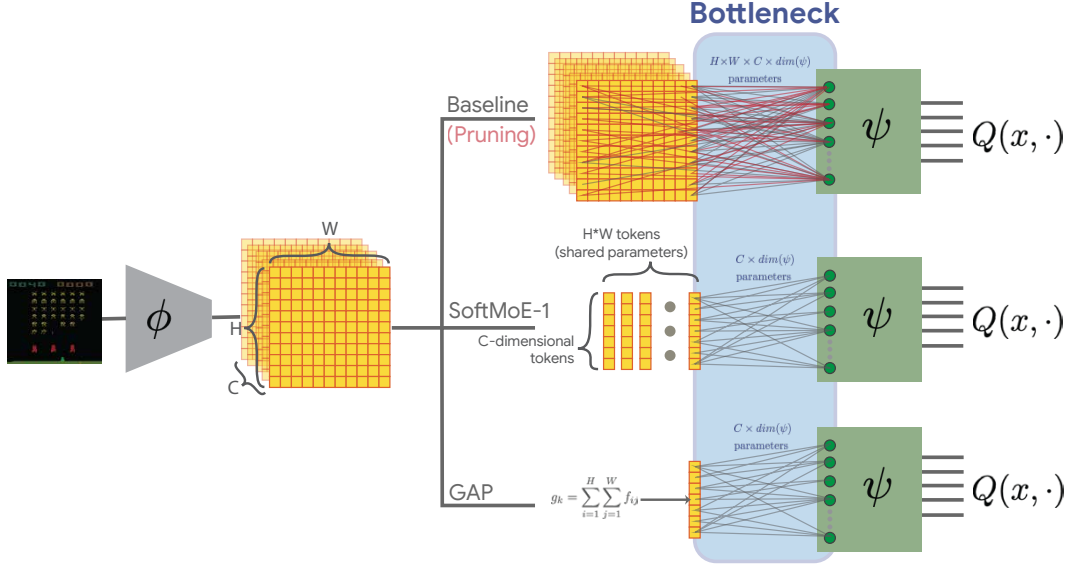


Figure 1 | Illustration of the bottleneck in pixel-based networks. Standard dense networks (**Baseline**) connect all ϕ outputs with ψ , resulting in $H \times W \times C \times \dim(\psi)$ parameters (scaled down when using **pruning**, shown in red). **SoftMoE-1** converts ϕ 's outputs into $H \times W$ tokens of dimension C ; the sharing of learned parameters across tokens results in a bottleneck with $C \times \dim(\psi)$ parameters. **GAP** performs average pooling across $H \times W$ spatial dimensions, resulting in C feature maps and $C \times \dim(\psi)$ parameters in the bottleneck.

performance gains are mostly due to a well-structured bottleneck, rather than the recently proposed architectural modifications to ψ . This insight suggests that simpler architectural interventions may be just as effective, which we demonstrate by using global average pooling (GAP) as an effective mechanism for enabling improved performance from scaling.

Our contributions can be summarized as follows: (i) We investigate the challenges leading to the performance degradation of scaled RL networks; (ii) we study the underlying reasons behind the success of existing architectural approaches in scaling; and (iii) we present pooling as a faster, simpler method yielding superior performance. We begin in Section 2 by providing the necessary background on Reinforcement Learning (RL), detailing the architecture employed in pixel-based deep RL, and outlining architectural modifications proposed by recent methods for addressing scaling challenges. Section 3.1 then describes our experimental setup. Our analyses investigating the difficulties of scaling RL networks and how existing methods attempt to address them are presented in Sections 3.2 and 3.3, respectively. Section 4 is dedicated to our results and analysis on RL networks with GAP. Finally, Section 5 covers the related work, followed by a conclusion and discussion in Section 6.

2. Preliminaries

2.1. Reinforcement learning

Reinforcement learning (RL) involves an agent moving through a series of states $x \in \mathcal{X}$ by selecting an action $a \in \mathcal{A}$ at discrete timesteps. After selecting action a_t from state x_t , the agent will receive a reward $r_t(x_t, a_t)$, and its goal is to maximize the discounted sum of cumulative rewards $\sum_{t=0}^{\infty} \gamma^t r_t$, where $\gamma \in [0, 1)$ by finding an optimal *policy* $\pi : \mathcal{X} \rightarrow \Delta(\mathcal{A})$ which quantifies the agent's behavior at each state. Value-based methods (Sutton and Barto, 1998) maintain estimates of the value of selecting action a from state x and following π afterwards: $Q(x, a) := \sum_{t=0}^{\infty} [\gamma^t r_t(x_t, a_t) | x_0 = x, a_0 = a, a_t \sim \pi(x_t)]$,

where π is induced from Q , for instance with the use of softmax: $\pi(x)(a) := \frac{e^{Q(x,a)}}{\sum_{a' \in \mathcal{A}} e^{Q(x,a')}}.$

Mnih et al. (2015) demonstrated deep neural networks can be very effective at approximating Q -values, even for complex domains such as Atari games (Bellemare et al., 2013); their network has served as the backbone for most deep RL network. Later, Espeholt et al. (2018) proposed using ResNet based architecture which demonstrates significant performance improvements over the original CNN architecture. For pixel-based environments, this family of networks consists of a set of convolutional layers (Fukushima, 1980), which we will collectively refer to as ϕ (and often referred to as the *encoder* or *representation*), followed by a set of dense layers, which we will collectively refer to as ψ . Thus given an input x , the network approximates the Q -values as $\tilde{Q}(x, \cdot) = \psi(\phi(x))$.

The output of ϕ is a 3-dimensional tensor $H \times W \times C$, where H is height, W is width, and C is the number of feature maps (channels); this output is typically flattened before being fed to ψ . Thus, the number of parameters for the functional composition $\psi \circ \phi$ is equal to $H \times W \times C \times \dim(\psi)$, where $\dim(\psi)$ is the dimensionality of the first dense layer in ψ . We refer to connection between ϕ and ψ as the **bottleneck**, and it will be the focus of most of our work. See Figure 1 for an illustration.

2.2. SoftMoE

Obando Ceron* et al. (2024) proposed replacing the dense layer in ψ with mixture-of-experts (MoEs). The input to the mixture is a set of tokens created by restructuring the 3-dimensional output of ϕ . Their investigation into different tokenization strategies revealed that forming $H \times W$ tokens of C dimensions achieved the highest performance. This reduces the number of parameters of the bottleneck to $C \times \dim(\psi)$. Sokar et al. (2025) demonstrated that tokenizing the output of ψ is a core source of the performance improvements of MoEs in RL and single expert (SoftMoE-1) has a close performance to using multiple experts across different scales.

2.3. Sparse Methods

Sokar et al. (2022) demonstrated that using sparse neural networks instead of dense networks increases learning speed and leads to improved performance. Graesser et al. (2022) studied different ways to induce sparsity in the network including pruning the network weights during training and using sparse networks from scratch. With a sparsity level s , the number of parameters in the bottleneck is $s \times H \times W \times C \times \dim(\psi)$. Recently (Obando Ceron et al., 2024) demonstrated that pruning is an effective approach that enables scaling networks. Below we will explain how these approaches change the architecture of the network.

Gradual pruning The training starts with a dense network and the low magnitude parameters are progressively pruned throughout training under a polynomial schedule (Zhu and Gupta, 2017). At the end iteration of pruning, the network will reach the target sparsity which is kept fixed during the rest of training.

Sparse from scratch A sparse neural network is defined at initialization with specific sparsity level that is maintained throughout training. The sparse topology is either fixed known as *static*, or dynamically optimized during training through a periodic change of a portion of the connections as proposed in RigL (Evci et al., 2020).

3. Analyses

Main hypothesis

A low-dimensional and well-structured **bottleneck** enables scaling deep RL networks.

We conduct a series of analyses, both quantitative and qualitative, to provide evidence for our main hypothesis. We investigate impacts on performance, plasticity, and properties of the learned features. Given the effectiveness of SoftMoEs (Obando Ceron* et al., 2024), Pruning (Obando Ceron et al., 2024), and Tokenization (Sokar et al., 2025) for scaling value-based networks, our analyses in this section will focus on these.

3.1. Experimental setup

Architectures We use the Impala architecture (Espeholt et al., 2018), as it has been demonstrated to yield stronger performance than the original architecture of Mnih et al. (2015). Our main experiments and analyses show results across different scales for the width of ψ ($\times 1$, $\times 2$, $\times 4$, $\times 8$). When a scale is not explicitly stated, our analysis defaults to the $\times 4$ scale due to its observed high gain (Obando Ceron et al., 2024; Obando Ceron* et al., 2024; Sokar et al., 2025). Following (Obando Ceron* et al., 2024; Sokar et al., 2025), we only scale ψ , unless specified otherwise. While our main focus is on the more performant ResNet backbone of Impala, we also demonstrate the broader applicability of our findings using a standard CNN architecture (Mnih et al., 2015).

Agents and environments We use the Rainbow agent (Hessel et al., 2018) and evaluate on the Arcade Learning Environment (ALE) suite (Bellemare et al., 2013) using the same 20 Atari games used by Obando Ceron* et al. (2024) and Sokar et al. (2025). Moreover, we present our main results on the full suite of 60 games. We ran each experiment for a total of 200 million environment steps, with 5 independent seeds, except for the experiments with an increased replay ratio of 2, where we report the results at 50M steps. Moreover, we evaluate Rainbow on the Procgen (Cobbe et al., 2019) benchmark and on the 100k benchmark (Łukasz Kaiser et al., 2020) using DER (the version of Rainbow tuned for this setting).

Code and compute resources For all our experiments, we use the Dopamine library¹ with Jax implementations (Castro et al., 2018). For SoftMoE (Obando Ceron* et al., 2024), we use the official implementation integrated in Dopamine. For the sparse methods (Graesser et al., 2022; Obando Ceron et al., 2024), we use the same JaxPruner library² (Lee et al., 2024) used by (Obando Ceron et al., 2024). All libraries have Apache-2.0 license. All experiments were run on NVIDIA Tesla P100 GPUs. The duration of each experiment ranged from 4 to 13 days, depending on the specific scale and algorithm. We present the exact run time for each case in Section 4.

Implementation details For all algorithms, we use the default hyperparameters in the Dopamine library. For sparse-training algorithms, we follow (Graesser et al., 2022) and use 90% sparsity. For gradual pruning, we start pruning at 8M environment steps and stop at 160M (80% into training), following the recommendation of Graesser et al. (2022); Obando Ceron et al. (2024). For RigL (Evci et al., 2020), we use a drop fraction of 20% and an update interval of 5000. For SoftMoE,

¹Dopamine: <https://github.com/google/dopamine>

²JaxPruner: <https://github.com/google-research/jaxpruner>

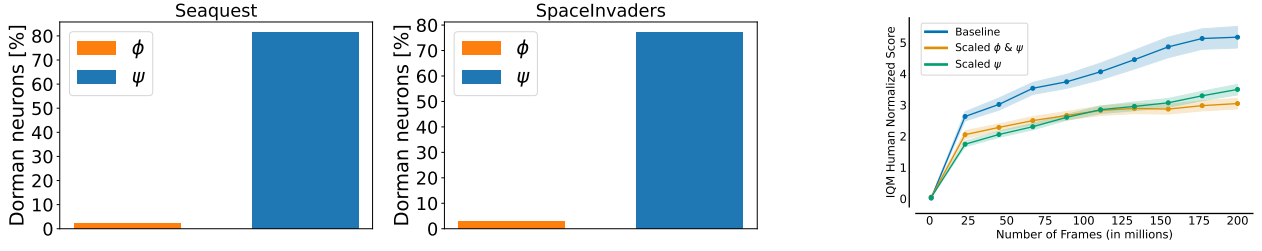


Figure 2 | **(Left)** Distribution of dormant neurons across ϕ and ψ in scaled baseline across different games at the end of training. The fully connected layer exhibits the highest percentage of dormancy. **(Right)** The performance degradation associated with scaling the entire network architecture is similar to that observed when only the bottleneck is scaled.

we use SoftMoE-1 not only because it has been shown to have a similar performance as standard SoftMoE (Sokar et al., 2025), but also to ensure we have a similar architecture as the other methods considered. We report interquartile mean (IQM) with 95% stratified bootstrap confidence intervals as recommended in (Agarwal et al., 2021). Full experimental details are provided in the appendix.

3.2. Why scaling deep RL networks hurts performance

As has been previously demonstrated, naïvely scaling networks deteriorates performance (Nauman et al., 2024; Obando Ceron et al., 2024; Obando Ceron* et al., 2024). In this section we conduct a series of experiments to diagnose the underlying causes for this difficulty.

We start by analyzing the training dynamics of a network where all layers within ϕ and ψ are scaled by a factor of 4. We examine neuron activity by measuring the fraction of dormant neurons (Sokar et al., 2023), which is an indicator of plasticity. We find that ψ exhibits a large fraction of dormant neurons, while ϕ has low dormancy rates, as shown in the left plot of Figure 2. This suggests that **scaling mostly affects the plasticity of the bottleneck**.

In the right plot of Figure 2, we compare the performance of the **baseline network** against the same network with **scaled ϕ and ψ** . As consistently observed in previous studies, the scaled network exhibits a degradation in performance. To investigate the contribution of ψ in this performance decrease, we only **scale the bottleneck** (via the first layer of ψ) to match the parameter count of the **fully scaled network**. As can be observed, the performance of the two scaled models is nearly identical, suggesting that **the bottleneck drives most of the performance degradation when scaling**.

To interpret the quality of the learned features of the scaled network, we generate saliency maps for the areas that have the greatest impact on the scaled network’s output using Grad-CAM (Selvaraju et al., 2017). Figure 3 (left) reveals that naïvely scaled networks fail to focus on important regions and focus on irrelevant background areas. This suggests that **scaling the bottleneck impairs a network’s ability to process and learn effective combinations of the representation ϕ** .

To further investigate potential challenges in feature learning within ψ , we study the network behavior when providing higher-level features to ψ . Specifically, we increased the depth of ϕ by adding four additional ResNet blocks, while using the scaled bottleneck. This modification makes ψ receive more structured, high-level features from the encoder. We present the performance throughout training in Figure 4. The fact that we observe a dramatic increase in performance suggests that **structured representations helps feature learning in scaled networks**.

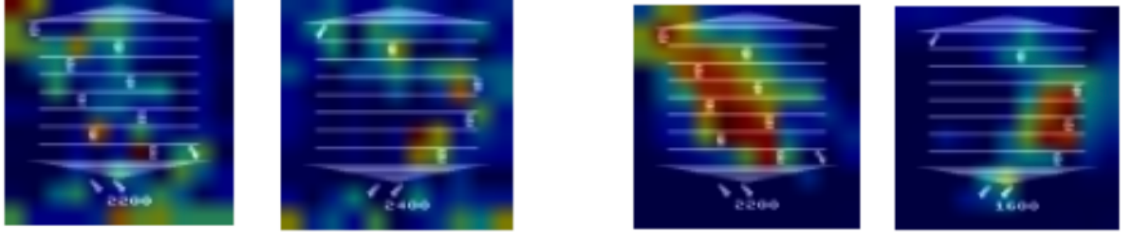


Figure 3 | **GAP helps improve attention to relevant areas of input.** Visualizing influential regions for network decisions using Grad-CAM (Selvaraju et al., 2017). (Left) The scaled baseline fails to attend to the important regions, focusing on irrelevant background details. (Right) GAP attends to the important regions in the input.

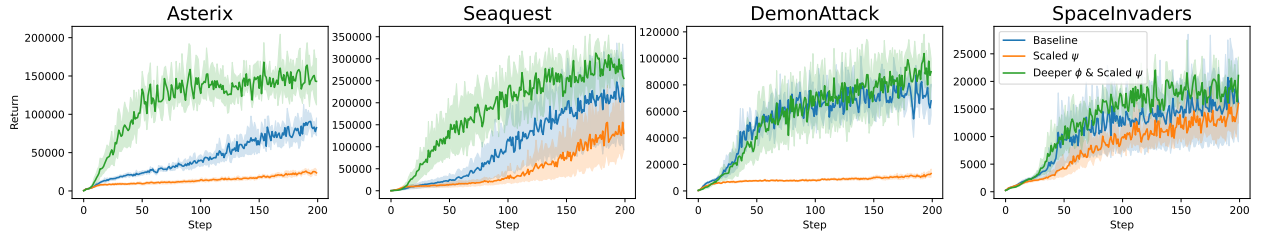


Figure 4 | Scaling ψ hinders learning effective combinations of encoder’s features, leading to significant performance drop. However, performance dramatically improves when the scaled ψ is fed with higher-level, more abstract features obtain by increasing the depth of ϕ .

3.3. Existing techniques are mainly targeting the bottleneck

As previously mentioned, there have been a number of recent proposals to enable scaling deep RL networks by using sophisticated architectural modifications. We hypothesize that a core reason for their effectiveness is that they are implicitly targeting the bottleneck. The strong performance of SoftMoE-1 and tokenized baselines presented by Sokar et al. (2025) support this claim, as they are primarily re-structuring the encoder output.

To validate our hypothesis on sparse methods, we evaluated the impact of sparse training techniques when limited to the bottleneck, while keeping all other layers dense. We performed this analysis on gradual pruning (Obando Ceron et al., 2024), dynamic sparsity (RigL) and static sparsity (Graesser et al., 2022; Sokar et al., 2022). As shown in the left plot of Figure 5, restricting sparsification to the scaled bottleneck results in improved performance across all sparse training techniques. This suggests that **applying sparsity only to the bottleneck is sufficient to enable scaling RL networks.**

In addition to structuring the encoder output, existing techniques effectively reduce the dimensionality of the bottleneck by either structuring the output as tokens (as in SoftMoE) which results in a lower dimensional input to ψ , or explicitly masking the majority of input weights (as in sparse methods). The right plot of Figure 5 confirms this reduction in parameters, and illustrates a positive correlation between scale and performance, which is notably absent in the baseline. This suggests that **low-dimensional and structured bottlenecks facilitate scaling deep RL networks.**

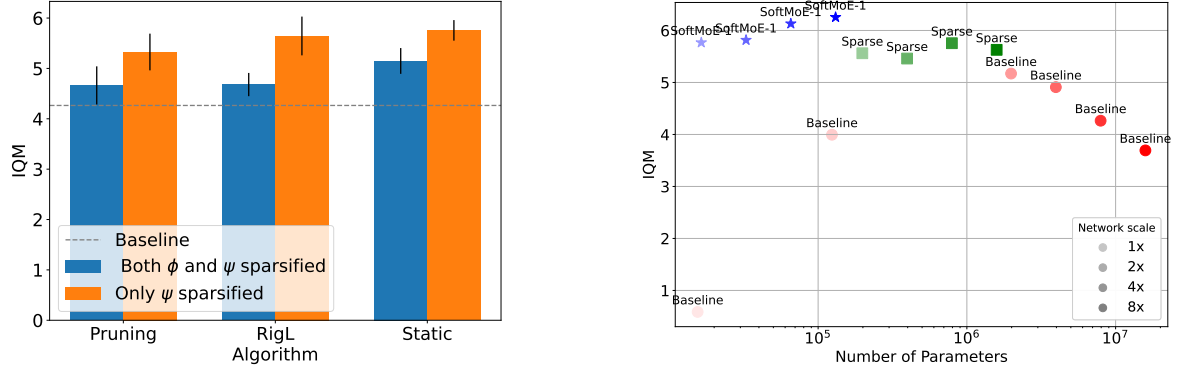


Figure 5 | **(Left)** Across different sparse algorithms, sparsification of only ψ yields better performance than sparsifying ϕ and ψ . **(Right)** The relation between performance and the effective number of parameters in ψ for different approaches. Architectural methods have lower effective density than the baseline which correlates with the observed performance improvements.

4. Mind the GAP!

Having identified low-dimensional and well-structured bottlenecks as the main factor enabling scaling networks, we demonstrate a *simple* alternative to the more sophisticated techniques recently explored: global average pooling (GAP) (Lin et al., 2013). We demonstrate its efficacy across wide range of settings and aspects, including: (1) *effectiveness* in network scaling under different scales, architectures, and in sample-efficient regime with high replay ratios (Figure 6); (2) improved training *stability* and feature learning (Figure 7); (3) unlocking *width and depth* scaling (Figure 8); (4) *computational efficiency* (Figure 9); and (5) *generalized gains* across various domains (Figure 11).

Simple The output feature maps of ϕ , denoted as $F \in \mathbb{R}^{H \times W \times C}$, are processed by average pooling. For each feature map (F^c), GAP computes the average over its spatial dimensions, resulting in the output ($g \in \mathbb{R}^C$), which is then fed to the fully connected layers ψ (see Figure 1 for an illustration):

$$g^c = \frac{1}{H \times W} \sum_{i=1}^H \sum_{j=1}^W F_{ij}^c. \quad (1)$$

Effective We evaluate the impact of this architectural change on various settings. *Scale*: We assess the performance of GAP across different network scales. The left plot of Figure 6 demonstrates that

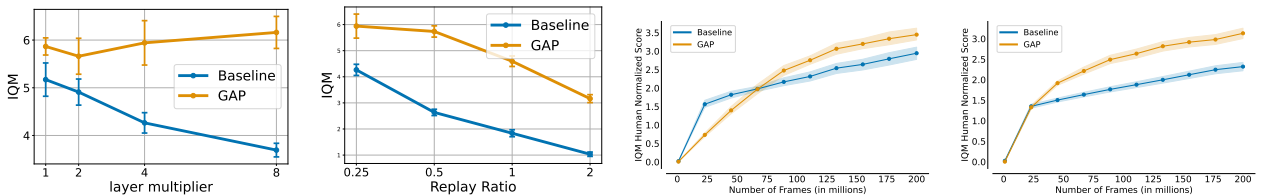


Figure 6 | The impact of GAP across wide range of setting. From left to right: performance across different network scales, sample-efficient training with various high replay ratio values (default = 0.25), performance of the smaller CNN used by (Mnih et al., 2015), and performance on the full 60 games of Atari 2600. In all cases, GAP significantly improves performance.

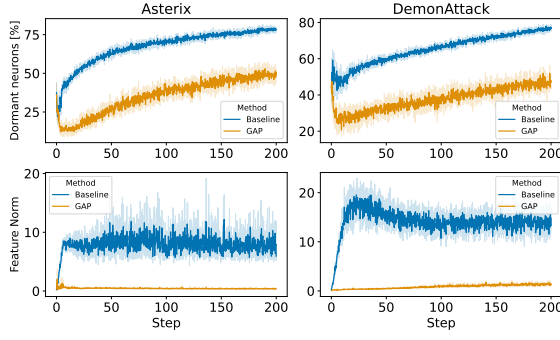


Figure 7 | Scaled networks with GAP exhibit less dormant neurons than the baseline and have lower feature norm.

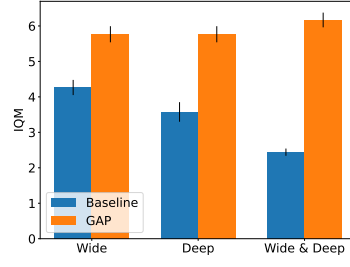


Figure 8 | Impact of scaling network depth and width. Increasing depth hurts performance for the baseline networks, and scaling both width and depth makes it even worse. GAP, however, unlocks scaling even for increased network depth, leading to significant performance gains.

this simple architectural change unlocks scaling in RL networks, leading to significant performance improvements across different scales. *Sample-efficient regime*: increasing the number of gradient updates per environment interaction (replay ratio) is favorable for sample-efficiency. Yet, higher replay ratios often hurt performance (Nikishin et al., 2022). We study the performance of the scaled network across varying the replay ratio values (default = 0.25). We find that even in this challenging setting, GAP has very strong performance against the baseline, yielding more sample-efficient agents, as shown in the center left plot of Figure 6. *Varying architecture*: we evaluate the effect of GAP on a different architecture for ϕ : the original CNN architecture used in (Mnih et al., 2015). The right center plot in Figure 6 shows that GAP can also provide performance gain to this architecture. *Full suite*: we assess the generalization of our findings beyond the 20 games used for most results and evaluate on the full set of 60 games of Atari. The rightmost plot of Figure 6 confirms that GAP consistently improves performance on the full suite.

Stable training dynamics Figure 3 (right) displays the saliency maps when training with GAP, where the network seems to be attending to the most important and relevant areas of the input. We further examine the dormant neurons (Sokar et al., 2023) and the norm of the features in Figure 7. We observe that the network exhibits fewer dormant neurons than the baseline and lower feature norms, suggesting improved plasticity and training stability.

Efficient In Figure 9 we report the total number of GPU hours per game for every scale, to compare the computational cost of the different methods. While scaling the baseline increases computational costs and degrades the performance, applying GAP to the encoder’s output reduces the effective density of ψ (and hence computational cost), while yielding performance

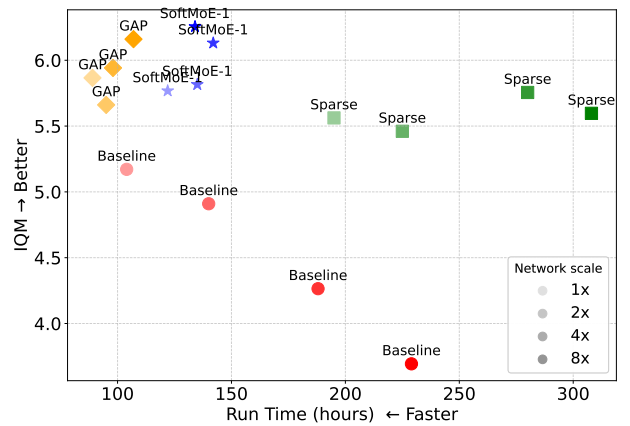


Figure 9 | The computational cost versus performance across varying network scales for different algorithms. GAP offers the *highest* speed while obtaining substantial performance improvements.

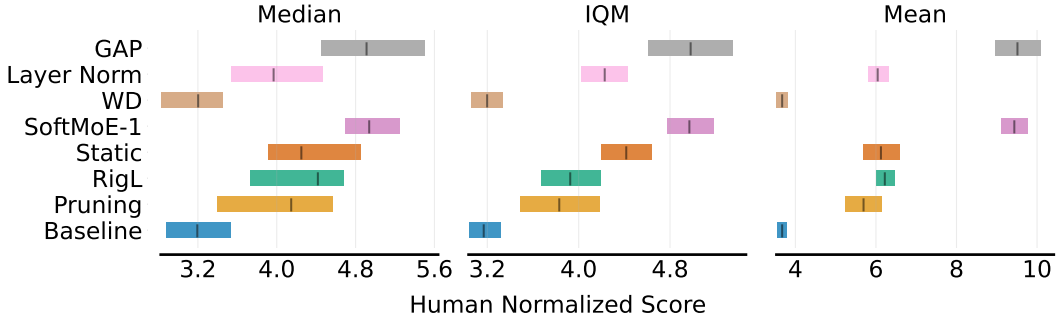


Figure 10 | Comparison against architectural and algorithmic techniques for scaling RL networks. We report Median, IQM, and Mean scores (Agarwal et al., 2021) at 100M environment steps. GAP presents a notably simpler alternative to the baseline approaches, while achieving the best performance.

gains. Despite having a similar effective density to SoftMoE, GAP’s inherent simplicity makes it more efficient by avoiding the extra computations associated with SoftMoE’s token construction and post-MoE projection. The high runtime observed in sparse methods, despite their low effective density, stems from the fact that sparsity is only simulated with parameter masking (Evci et al., 2020; Hoefler et al., 2021; Mocanu et al., 2018).

Unlocking width-depth scaling We demonstrate the effectiveness of GAP in scaling network width which is the focus of previous works (Obando Ceron et al., 2024; Obando Ceron* et al., 2024; Sokar et al., 2025). Beyond this, we also explore how increasing network depth, or both width and depth, impacts the performance of RL networks. Specifically, we add extra fully connected layer in ψ and evaluate the performance with both unscaled and scaled ψ . We present the results in Figure 8. We find that the baseline’s performance drops with increased network depth, worsening significantly when scaling both dimensions. In contrast, interestingly GAP maintains strong performance across all scaling dimensions, confirming the impact of the representation learned by the bottleneck in the overall performance of the network.

Comparison against other methods We compare the performance of GAP against various architectural techniques including pruning (Obando Ceron et al., 2024), static and dynamic sparsity (RigL) (Graesser et al., 2022), and SoftMoE-1 (Sokar et al., 2025). Moreover, we include a comparison against algorithmic methods including weight decay (Obando Ceron et al., 2024; Sokar et al., 2023), and layer normalization (Nauman et al., 2024). Figure 10 shows that GAP outperforms all other methods, demonstrating its effectiveness, despite its simplicity.

Generalization to other domains We evaluate Rainbow on Procgen (Cobbe et al., 2019) and DER (Van Hasselt et al., 2019) on Atari100K (Łukasz Kaiser et al., 2020). Consistent with our previous findings, we observe that GAP significantly improves performance of scaled networks in those domains as demonstrated in Figure 11.

5. Related Work

Several works have shown that scaling RL network causes substantial performance degradation due to training instabilities exhibited by the network (Bjorck et al., 2021; Hessel et al., 2018; Obando Ceron* et al., 2024). Although the precise causes of these issues remain unclear, several approaches aim to

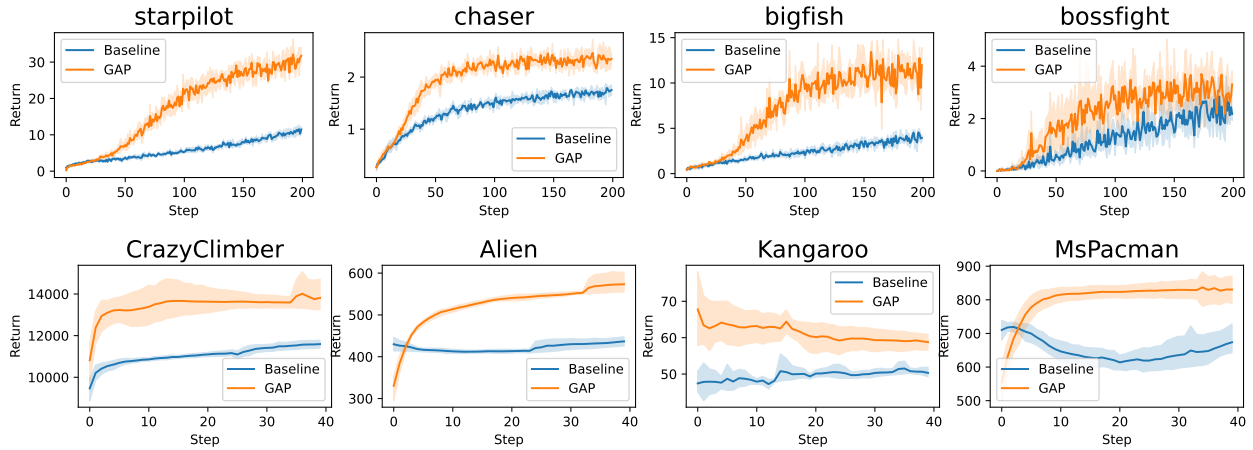


Figure 11 | Performance for Rainforest on Procgen (Cobbe et al., 2019) (top) and DER on Atari100K (Łukasz Kaiser et al., 2020) (bottom). GAP leads to performance gains for scaled networks in diverse domains.

mitigate them. We categorize these methods to architectural methods that alter the standard network architecture and algorithmic methods.

Scaling through architectural changes Obando Ceron* et al. (2024) integrated a Mixture-of-Experts (MoE) following the encoder in single-task RL networks. Their results across multiple domains highlight the effectiveness of this approach for scaling RL, with SoftMoE (Puigcerver et al., 2024) outperforming traditional MoE Shazeer et al. (2017). Willi* et al. (2024) further demonstrate the applicability of MoE in the multi-task setting. Sokar et al. (2025) show that replacing the flattened representation of the encoder by tokenized representation that preserves the spatial structure improves performance of scaled networks. Another line of research studies replacing dense parameters by sparse ones in both online (Graesser et al., 2022; Sokar et al., 2022; Tan et al., 2023) and offline RL (Arnob et al., 2021). This approach has demonstrated its effectiveness in increasing the learning speed and performance of RL agents. Network sparsity is achieved either by starting with a dense network and progressively pruning weights, or by initializing with a sparse network and maintaining a consistent sparsity level throughout training. In the latter case, the sparse structure can be kept static or optimized dynamically during training using methods like SET (Mocanu et al., 2018) and RigL (Evci et al., 2020). Recently, Obando Ceron et al. (2024) showed that gradual magnitude pruning helps in scaling RL networks, leading to improved performance. Concurrent works have independently proposed similar approaches to GAP (Kooi et al., 2025; Trumpp et al., 2025), which provides extra evidence for the efficacy of this method.

Scaling through algorithmic changes Bjorck et al. (2021) show that using spectral normalization (Miyato et al., 2018) helps to improve training stability and enable using large neural networks for actor-critic methods. Farebrother et al. (2023a) explore the usage of auxiliary tasks to learn scaled representations. Schwarzer* et al. (2023) propose several tricks to enable scaling including weight decay, network reset, increased discount factor, among others. Farebrother et al. (2024) demonstrated that training value networks using classification with categorical cross-entropy, as opposed to regression, leads to better performance in scaled networks. Nauman et al. (2024) employ layer normalization (Ba et al., 2016), weight decay, and weight reset (Nikishin et al., 2022).

6. Conclusion

Recent proposals for enabling scaling in deep reinforcement learning have relied on sophisticated architectural interventions, such as the use of mixtures-of-experts and sparse training techniques. We demonstrated that these methods are indirectly targeting the **bottleneck** connecting the encoder ϕ and dense layers ψ , in a standard deep RL network. A consequence of our analyses is that directly targeting this bottleneck, for instance with global average pooling, can achieve the same (or higher) performance gains.

Our work highlights the importance of better understanding the training dynamics of neural networks in the context of reinforcement learning. The fact that a simple technique like global average pooling can outperform existing literature suggests that architecture design is ripe for exploration. There is also a likely connection of our findings with works exploring representation learning for RL (Castro et al., 2021; Farebrother et al., 2023b; Kemertas and Aumentado-Armstrong, 2021; Zhang et al., 2021), given that these generally target the output of ϕ ; indeed, most of these methods aim to *structure* the outputs of ϕ so as to improve the generalizability and efficiency of the networks. It would be valuable to investigate whether approaches like GAP are complementary with (and ideally help enhance) more sophisticated representation learning approaches.

Limitations Although our broad set of results suggest our findings are quite general, our investigation has focused on pixel-based environments where there is a clear bottleneck, or separation between ϕ (the convolutional layers) and ψ (the fully connected layers). It is not clear whether our findings extend to non-pixel based environments or architectures where there isn't a clear bottleneck, but would be an interesting line of future work.

Acknowledgements

The authors would like to thank Gheorghe Comanici, Joao Madeira Araujo, Karolina Dziugaite, Doina Precup, and the rest of the Google DeepMind team, as well as Roger Creus Castanyer and Johan Obando-Ceron, for valuable feedback on this work.

References

- R. Agarwal, M. Schwarzer, P. S. Castro, A. C. Courville, and M. Bellemare. Deep reinforcement learning at the edge of the statistical precipice. In M. Ranzato, A. Beygelzimer, Y. Dauphin, P. Liang, and J. W. Vaughan, editors, *Advances in Neural Information Processing Systems*, volume 34, pages 29304–29320. Curran Associates, Inc., 2021.
- S. Y. Arnob, R. Ohib, S. Plis, and D. Precup. Single-shot pruning for offline reinforcement learning. *arXiv preprint arXiv:2112.15579*, 2021.
- J. L. Ba, J. R. Kiros, and G. E. Hinton. Layer normalization. *arXiv preprint arXiv:1607.06450*, 2016.
- M. G. Bellemare, Y. Naddaf, J. Veness, and M. Bowling. The arcade learning environment: An evaluation platform for general agents. *Journal of Artificial Intelligence Research*, 47:253–279, 2013.
- M. G. Bellemare, S. Candido, P. S. Castro, J. Gong, M. C. Machado, S. Moitra, S. S. Ponda, and Z. Wang. Autonomous navigation of stratospheric balloons using reinforcement learning. *Nature*, 588(7836): 77–82, 2020.
- N. Bjorck, C. P. Gomes, and K. Q. Weinberger. Towards deeper deep reinforcement learning with spectral normalization. *Advances in neural information processing systems*, 34:8242–8255, 2021.
- P. S. Castro, S. Moitra, C. Gelada, S. Kumar, and M. G. Bellemare. Dopamine: A research framework for deep reinforcement learning. *arXiv preprint arXiv:1812.06110*, 2018.
- P. S. Castro, T. Kastner, P. Panangaden, and M. Rowland. MICO: Improved representations via sampling-based state similarity for markov decision processes. In A. Beygelzimer, Y. Dauphin, P. Liang, and J. W. Vaughan, editors, *Advances in Neural Information Processing Systems*, 2021. URL <https://openreview.net/forum?id=wFp6kmQELgu>.
- K. Cobbe, C. Hesse, J. Hilton, and J. Schulman. Leveraging procedural generation to benchmark reinforcement learning. *arXiv preprint arXiv:1912.01588*, 2019.
- J. Degraeve, F. Felici, J. Buchli, M. Neunert, B. Tracey, F. Carpanese, T. Ewalds, R. Hafner, A. Abdolmaleki, D. de las Casas, C. Donner, L. Fritz, C. Galperti, A. Huber, J. Keeling, M. Tsimpoukelli, J. Kay, A. Merle, J.-M. Moret, S. Noury, F. Pesamosca, D. Pfau, O. Sauter, C. Sommariva, S. Coda, B. Duval, A. Fasoli, P. Kohli, K. Kavukcuoglu, D. Hassabis, and M. Riedmiller. Magnetic control of tokamak plasmas through deep reinforcement learning. *Nature*, 602(7897):414–419, 2022.
- L. Espeholt, H. Soyer, R. Munos, K. Simonyan, V. Mnih, T. Ward, Y. Doron, V. Firoiu, T. Harley, I. Dunning, et al. Impala: Scalable distributed deep-rl with importance weighted actor-learner architectures. In *Proceedings of the International Conference on Machine Learning (ICML)*, 2018.
- U. Evci, T. Gale, J. Menick, P. S. Castro, and E. Elsen. Rigging the lottery: Making all tickets winners. In *International conference on machine learning*, pages 2943–2952. PMLR, 2020.
- J. Farebrother, J. Greaves, R. Agarwal, C. L. Lan, R. Goroshin, P. S. Castro, and M. G. Bellemare. Proto-value networks: Scaling representation learning with auxiliary tasks. In *The Eleventh International Conference on Learning Representations*, 2023a. URL <https://openreview.net/forum?id=oGDKSt9JrZi>.
- J. Farebrother, J. Greaves, R. Agarwal, C. L. Lan, R. Goroshin, P. S. Castro, and M. G. Bellemare. Proto-value networks: Scaling representation learning with auxiliary tasks, 2023b. URL <https://arxiv.org/abs/2304.12567>.

- J. Farebrother, J. Orbay, Q. Vuong, A. A. Taiga, Y. Chebotar, T. Xiao, A. Irpan, S. Levine, P. S. Castro, A. Faust, et al. Stop regressing: Training value functions via classification for scalable deep rl. In *International Conference on Machine Learning*, pages 13049–13071. PMLR, 2024.
- K. Fukushima. Neocognitron: A self-organizing neural network model for a mechanism of pattern recognition unaffected by shift in position. *Biological Cybernetics*, 36(4):193–202, 1980.
- L. Graesser, U. Evci, E. Elsen, and P. S. Castro. The state of sparse training in deep reinforcement learning. In *International Conference on Machine Learning*, pages 7766–7792. PMLR, 2022.
- M. Hessel, J. Modayil, H. V. Hasselt, T. Schaul, G. Ostrovski, W. Dabney, D. Horgan, B. Piot, M. G. Azar, and D. Silver. Rainbow: Combining improvements in deep reinforcement learning. In *AAAI*, 2018.
- T. Hoefler, D. Alistarh, T. Ben-Nun, N. Dryden, and A. Peste. Sparsity in deep learning: Pruning and growth for efficient inference and training in neural networks. *Journal of Machine Learning Research*, 22(241):1–124, 2021.
- M. Kemertas and T. Aumentado-Armstrong. Towards robust bisimulation metric learning. *CoRR*, abs/2110.14096, 2021. URL <https://arxiv.org/abs/2110.14096>.
- J. E. Kooi, Z. Yang, and V. François-Lavet. Hadamax encoding: Elevating performance in model-free atari, 2025.
- J. H. Lee, W. Park, N. E. Mitchell, J. Pilault, J. S. O. Ceron, H.-B. Kim, N. Lee, E. Frantar, Y. Long, A. Yazdanbakhsh, et al. Jaxpruner: A concise library for sparsity research. In *Conference on Parsimony and Learning*, pages 515–528. PMLR, 2024.
- M. Lin, Q. Chen, and S. Yan. Network in network. *CoRR*, abs/1312.4400, 2013. URL <http://arxiv.org/abs/1312.4400>.
- T. Miyato, T. Kataoka, M. Koyama, and Y. Yoshida. Spectral normalization for generative adversarial networks. In *International Conference on Learning Representations*, 2018.
- V. Mnih, K. Kavukcuoglu, D. Silver, A. A. Rusu, J. Veness, M. G. Bellemare, A. Graves, M. Riedmiller, A. K. Fidjeland, G. Ostrovski, S. Petersen, C. Beattie, A. Sadik, I. Antonoglou, H. King, D. Kumaran, D. Wierstra, S. Legg, and D. Hassabis. Human-level control through deep reinforcement learning. *Nature*, 518(7540):529–533, Feb. 2015.
- D. C. Mocanu, E. Mocanu, P. Stone, P. H. Nguyen, M. Gibescu, and A. Liotta. Scalable training of artificial neural networks with adaptive sparse connectivity inspired by network science. *Nature communications*, 9(1):2383, 2018.
- M. Nauman, M. Ostaszewski, K. Jankowski, P. Miłoś, and M. Cygan. Bigger, regularized, optimistic: scaling for compute and sample efficient continuous control. In *The Thirty-eighth Annual Conference on Neural Information Processing Systems*, 2024. URL <https://openreview.net/forum?id=fu0xdh4aEJ>.
- E. Nikishin, M. Schwarzer, P. D’Oro, P.-L. Bacon, and A. Courville. The primacy bias in deep reinforcement learning. In *International conference on machine learning*, pages 16828–16847. PMLR, 2022.
- J. S. Obando Ceron, A. Courville, and P. S. Castro. In value-based deep reinforcement learning, a pruned network is a good network. In *Proceedings of the 41st International Conference on Machine Learning*, volume 235 of *Proceedings of Machine Learning Research*, pages 38495–38519. PMLR, 21–27 Jul 2024.

- J. S. Obando Ceron*, G. Sokar*, T. Willi*, C. Lyle, J. Farebrother, J. N. Foerster, G. K. Dziugaite, D. Precup, and P. S. Castro. Mixtures of experts unlock parameter scaling for deep RL. In *Forty-first International Conference on Machine Learning*, 2024. URL <https://openreview.net/forum?id=X9VMhfFwn>.
- J. Puigcerver, C. R. Ruiz, B. Mustafa, and N. Houlsby. From sparse to soft mixtures of experts. In *The Twelfth International Conference on Learning Representations*, 2024.
- M. Schwarzer*, J. S. Obando Ceron*, A. Courville, M. G. Bellemare, R. Agarwal, and P. S. Castro. Bigger, better, faster: Human-level Atari with human-level efficiency. In A. Krause, E. Brunskill, K. Cho, B. Engelhardt, S. Sabato, and J. Scarlett, editors, *Proceedings of the 40th International Conference on Machine Learning*, volume 202 of *Proceedings of Machine Learning Research*, pages 30365–30380. PMLR, 23–29 Jul 2023.
- R. R. Selvaraju, M. Cogswell, A. Das, R. Vedantam, D. Parikh, and D. Batra. Grad-cam: Visual explanations from deep networks via gradient-based localization. In *Proceedings of the IEEE international conference on computer vision*, pages 618–626, 2017.
- N. Shazeer, A. Mirhoseini, K. Maziarz, A. Davis, Q. Le, G. Hinton, and J. Dean. Outrageously large neural networks: The sparsely-gated mixture-of-experts layer. In *International Conference on Learning Representations*, 2017. URL <https://openreview.net/forum?id=B1ckMDqlg>.
- G. Sokar, E. Mocanu, D. C. Mocanu, M. Pechenizkiy, and P. Stone. Dynamic sparse training for deep reinforcement learning. In *International Joint Conference on Artificial Intelligence*, 2022.
- G. Sokar, R. Agarwal, P. S. Castro, and U. Evci. The dormant neuron phenomenon in deep reinforcement learning. In *International Conference on Machine Learning*, pages 32145–32168. PMLR, 2023.
- G. Sokar, J. S. O. Ceron, A. Courville, H. Larochelle, and P. S. Castro. Don’t flatten, tokenize! unlocking the key to softmoe’s efficacy in deep RL. In *The Thirteenth International Conference on Learning Representations*, 2025. URL <https://openreview.net/forum?id=8oCr10aYcc>.
- R. S. Sutton and A. G. Barto. *Introduction to Reinforcement Learning*. MIT Press, Cambridge, MA, USA, 1st edition, 1998. ISBN 0262193981.
- Y. Tan, P. Hu, L. Pan, J. Huang, and L. Huang. Rlx2: Training a sparse deep reinforcement learning model from scratch. In *The Eleventh International Conference on Learning Representations*, 2023.
- R. Trumpp, A. Schäfftlein, M. Theile, and M. Caccamo. Impoola: The power of average pooling for image-based deep reinforcement learning. *arXiv preprint arXiv:2503.05546*, 2025.
- H. P. Van Hasselt, M. Hessel, and J. Aslanides. When to use parametric models in reinforcement learning? *Advances in Neural Information Processing Systems*, 32, 2019.
- O. Vinyals, I. Babuschkin, W. M. Czarnecki, M. Mathieu, A. Dudzik, J. Chung, D. H. Choi, R. Powell, T. Ewalds, P. Georgiev, J. Oh, D. Horgan, M. Kroiss, I. Danihelka, A. Huang, L. Sifre, T. Cai, J. P. Agapiou, M. Jaderberg, A. S. Vezhnevets, R. Leblond, T. Pohlen, V. Dalibard, D. Budden, Y. Sulsky, J. Molloy, T. L. Paine, C. Gulcehre, Z. Wang, T. Pfaff, Y. Wu, R. Ring, D. Yogatama, D. Wünsch, K. McKinney, O. Smith, T. Schaul, T. Lillicrap, K. Kavukcuoglu, D. Hassabis, C. Apps, and D. Silver. Grandmaster level in starcraft ii using multi-agent reinforcement learning. *Nature*, 575(7782): 350–354, 2019.
- T. Willi*, J. S. O. Ceron*, J. N. Foerster, G. K. Dziugaite, and P. S. Castro. Mixture of experts in a mixture of RL settings. In *Reinforcement Learning Conference*, 2024. URL <https://openreview.net/forum?id=5FF06R10Em>.

- P. R. Wurman, S. Barrett, K. Kawamoto, J. MacGlashan, K. Subramanian, T. J. Walsh, R. Capobianco, A. Devlic, F. Eckert, F. Fuchs, L. Gilpin, P. Khandelwal, V. Kompella, H. Lin, P. MacAlpine, D. Oller, T. Seno, C. Sherstan, M. D. Thomure, H. Aghabozorgi, L. Barrett, R. Douglas, D. Whitehead, P. Dürr, P. Stone, M. Spranger, and H. Kitano. Outracing champion gran turismo drivers with deep reinforcement learning. *Nature*, 602(7896):223–228, 2022.
- A. Zhang, R. T. McAllister, R. Calandra, Y. Gal, and S. Levine. Learning invariant representations for reinforcement learning without reconstruction. In *International Conference on Learning Representations*, 2021. URL <https://openreview.net/forum?id=-2FCwDKRREu>.
- M. Zhu and S. Gupta. To prune, or not to prune: exploring the efficacy of pruning for model compression. *arXiv preprint arXiv:1710.01878*, 2017.
- Łukasz Kaiser, M. Babaeizadeh, P. Miłoś, B. Osiński, R. H. Campbell, K. Czechowski, D. Erhan, C. Finn, P. Kozakowski, S. Levine, A. Mohiuddin, R. Sepassi, G. Tucker, and H. Michalewski. Model based reinforcement learning for atari. In *International Conference on Learning Representations*, 2020. URL <https://openreview.net/forum?id=S1xCPJHtDB>.

Table 1 | Hyper-parameters for Rainbow and DER agents.

		Atari	
	Hyper-parameter	Rainbow	DER
Training	Adam’s (ϵ)	1.5e-4	0.00015
	Adam’s learning rate	6.25e-5	0.0001
	Batch Size	32	32
	Weight Decay	0	0
Architecture	Activation Function	ReLU	ReLU
	Fully connected layer Width	512	512
Algorithm	Replay Capacity	1000000	1000000
	Minimum Replay History	20000	1600
	Number of Atoms	51	51
	Reward Clipping	True	True
	Update Horizon	3	10
	Update Period	4	1
	Discount Factor	0.99	0.99
	Exploration ϵ	0.01	0.01
	Sticky Actions	True	False

A. Experimental Details

Hyperparameter details We use the default hyperparameters for all the studied algorithms. We present the values of these parameters in Table 1. For the dormant neuron analysis, we use a dormancy threshold of 0.001. For the feature learning analysis (Figure 4), we increase the depth of the encoder by adding two ResNet blocks.

Atari Games (Bellemare et al., 2013) We use the set of 20 games used in Obando Ceron* et al. (2024); Sokar et al. (2025) for direct comparison. The set has the following games: Asterix, SpaceInvaders, Breakout, Pong, Qbert, DemonAttack, Seaquest, WizardOfWor, RoadRunner, BeamRider, Frostbite, CrazyClimber, Assault, Krull, Boxing, Jamesbond, Kangaroo, UpNDown, Gopher, and Hero. This set is used in most of our analysis, nevertheless we provide our main results on the full suite of 60 games.

Atari100K Games (Łukasz Kaiser et al., 2020) We test on the 26 games of this benchmark. It includes the following games: Alien, Amidar, Assault, Asterix, BankHeist, BattleZone, Boxing, Breakout, ChopperCommand, CrazyClimber, DemonAttack, Freeway, Frostbite, Gopher, Hero, Jamesbond, Kangaroo, Krull, KungFuMaster, MsPacman, Pong, PrivateEye, Qbert, RoadRunner, Seaquest, UpNDown.

B. Extra Experiments

B.1. Comparison against max pooling

We compare the performance of global average pooling with global max pooling for Rainbow on the set of 20 games. We find the GAP outperforms max pooling as demonstrated in Figure 12.

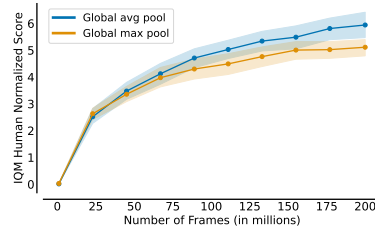


Figure 12 | Comparison between GAP and global max pooling for Rainbow.

We hypothesize this is due to GAP’s ability to retain more comprehensive information through its averaging operation.

B.2. Performance throughout training

[Figure 13](#) and [Figure 14](#) present the performance per game throughout training for Atari and Atari100K benchmarks, respectively.

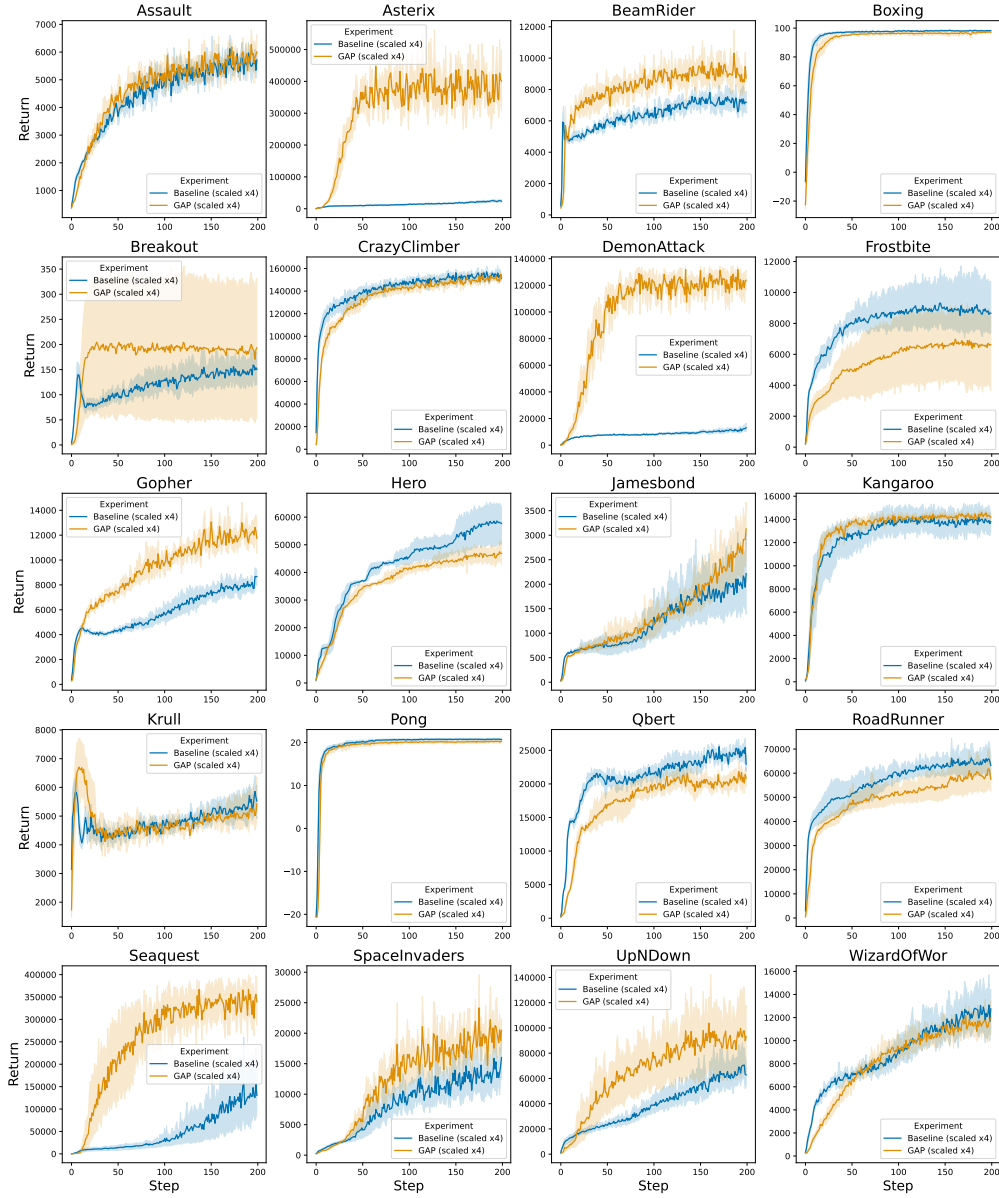


Figure 13 | Performance during training on the 20 games of the Atrai benchmark.

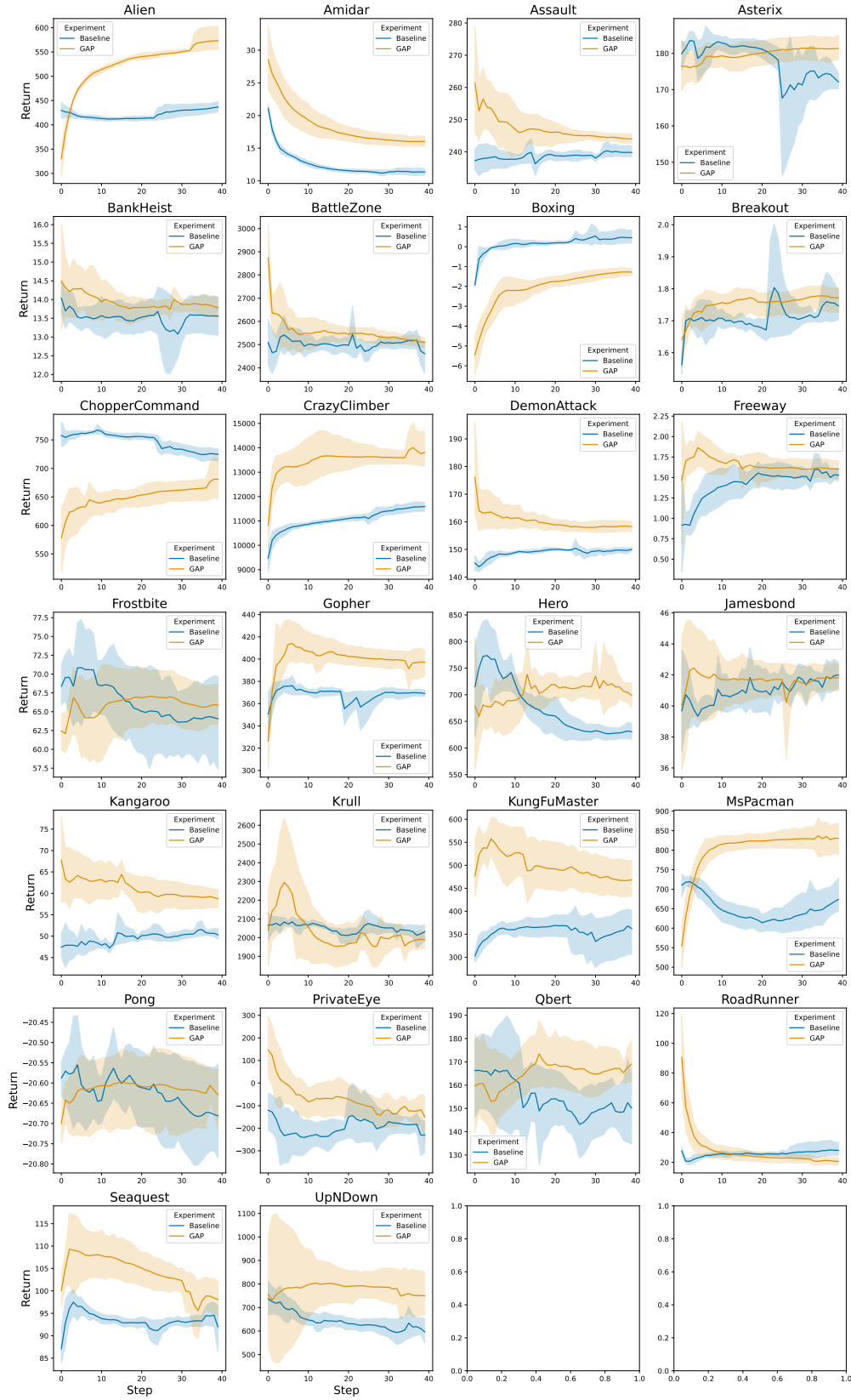


Figure 14 | Performance during training on the 26 games of the Atrai100k benchmark.